UNITECH 2022 GABROVO

INTERNATIONAL SCIENTIFIC CONFERENCE
18-19 November 2022, GABROVO

EFFECTS OF THE PROJECTILE POSITION INSIDE THE CARTRIGE AND CARTRIDGE THICKNESS ON THE COOK-OFF

Çiğdem Susantez[1], Kamil Kahveci[1], Oktay Hacıhafızoğlu[1], Hilmi Kuşçu[1]

[1] Trakya University Engineering Faculty Mechanical Engineering Department

Abstract

Cook-off is an undesired situation regarding the accuracy of the shot and accidents. In this study, effects of the thickness of the cartridge and projectile position inside the cartridge on the cook-off phenomena have been investigated numerically by Comsol Multiphysics and Simulation software. Results showed that generally increasing the thickness of the cartridge and placing projectile further back inside the cartridge prolongs the cook-off time.

Keywords: cook-off, barrel, cartridge.

INTRODUCTION

The power of the firearms shows the power of the armies. Inner ballistics is very important scientific field for the gun design. It models processes inside the barrel in inner ballistic time which is in miliseconds. Studies related to the gun barrel inner temperature and cook-off analysis is very important regarding the inner ballistics.

One of the undesired incident is the cook-off inside the barrel. It is the self-ignition of the propellant and may cause accidents. Işık and Göktaş [1] performed experimental and numerical study related the cook-off of a 7.62 mm rifle. They showed that shot number can be increased without cook-off by increasing the time between two magazines, wall thickness of the combustion chamber and cartridge case. Mishra et.al [2] proposed exponentially decaying heat flux for the numerical modelling of the temperature variation of 155mm gun barrel in their study. They also experimentally validated their model. Suyadnya et. al [3] suggested an experimentally validated numerical study on the heat transfer modelling of a 155mm cannon barrel. They presented the result that the maximum number of shots without cook-off is 27 in 294 seconds (time interval of 10 seconds for a shot and rest time of 6 seconds for every six shots). Akçay and Yükselen [4] applied their numerical, one-dimensional, unsteady heat transfer model on the 7.62mm M60 Machine gun barrel for sustained firing. They obtained convective heat transfer coefficient inside the barrel calculated by internal ballistics and considered temperature dependent gun barrel material in their study.

In this paper, we have numerically solved the unsteady heat transfer problem for the combustion chamber of a 7.62mm barrel during sustained firing. We have also investigated the effects of the cartridge thickness and projectile position inside the cartridge on the cook-off phenomena.

MATERIAL AND METHOD

Geometry of the investigated region of the combustion chamber is given in Fig. 1. The length of the investigated geometry of the combustion chamber (L) and cartridge (except from the thickness of the primer region which is 1.6mm) are 55 mm and 52.12mm (53.72mm-1.6mm) respectively. Geometric dimensions of the outer surface of the cartridge has been taken for 7.62x54mmR [5]. Geometric dimensions of the combustion chamber has also been obtained from the study of Işık and Göktaş [1] by using Web Plot Digitizer software. Lengths given in Fig. 1 are proportional, their dimensions have also been presented on Table 1.

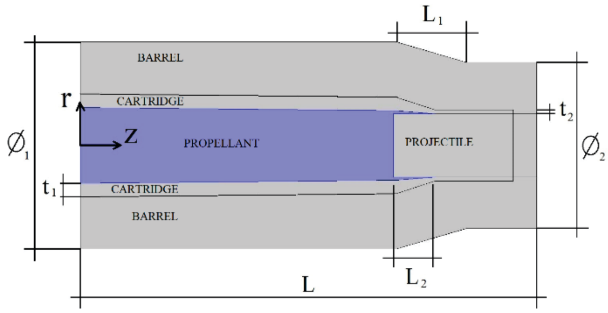

Fig. 1. *Combustion chamber with cartridge*

Table 1. *Dimensions of the investigated geometry*

Dimension	**Value (mm)**
L	55
L_1	8.4 [1]
L_2 Investigated parameter	0 and 5
t_1 Investigated parameter	1.6 and 2.4
t_2 measured	0.455
$\emptyset_1$	24.9 [1]
$\emptyset_2$	20 [1]

Constant thermopysical properties have been considered for the cartridge, barrel, projectile material and propellant. Thermophysical properties of the materials investigated in this study are presented on Table 2. Barrel is made of AISI 4140 steel [1], cartridge and projectile materials are brass and lead, respectively. WC846 is a popular propellant for the 7.62mm guns [6] and it contains 87% of Nitrocellulose [7]. Consequently, thermophysical properties of the projectile could be taken these of the Nitrocellulose.

Table 2. *Thermophysical properties*

Property	**Value**
Thermal conductivity of the barrel k_{steel} (W/mK)	37.7 [1]
Density of the barrel ρ_{steeel} (kg/m^3)	7850 [1]
Specific heat of the barrel c_{steeel} (J/kgK)	519 [1]
Thermal conductivity of the cartridge k_{brass} (W/mK)	111 [1]
Density of the cartridge ρ_{brass} (kg/m^3)	8600 [1]
Specific heat of the cartridge c_{brass} (J/kgK)	162 [1]
Thermal conductivity of the propellant $k_{propellant}$ (W/mK)	0.09 [7]
Density of the propellant $\rho_{propellant}$ (kg/m^3)	980 [8]
Specific heat of the propellant $c_{propellant}$ (J/kgK)	1109 [7]
Thermal conductivity of the projectile $k_{projectile}$ (W/mK)	34.7 [9]
Density of the projectile $\rho_{projectile}$ (kg/m^3)	11340 [10]
Specific heat of the projectile $c_{projectile}$ (J/kgK)	130 [11]

The governing equation for the model and related initial and boundary conditions are presented in Eqs. (1)-(7). Eqs (1)-(3) are valid for the whole domains (barrel, cartridge, projectile and propellant) with their thermophysical properties. Eqs. (4) is defined for the outside surface of combustion chamber.

$$\rho c \frac{\partial T}{\partial t} = \vec{\nabla} \cdot (k \vec{\nabla} T) \tag{1}$$

$$k \left. \frac{\partial T}{\partial z} \right|_{z=0} = 0 \tag{2}$$

$$-k \left. \frac{\partial T}{\partial z} \right|_{z=L} = 0 \tag{3}$$

$$\vec{n} \cdot (-k_{barrel} \vec{\nabla} T) = h_{out}(T - T_{out}) + \varepsilon\sigma(T^4 - {T_{out}}^4) \tag{4}$$

where ε, σ and h_{out} are the emissivity of the barrel surface (0.85), Stefan-Boltzmann constant (5.67·10^{-8}W/m^{2}K^4) and outside heat convective coefficient of the barrel (25W/m^{2}K), respectively [1]. Outside medium temperature T_{out} and initial temperature T_i are assumed to be 21°C.

$$T|_{t=0} = T_i \tag{5}$$

Eq. (6) is valid on the contact surfaces of the materials.

$$-k_i \frac{\partial T}{\partial n} = -k_j \frac{\partial T}{\partial n} \tag{6}$$

where i and j shows the corresponding material which are in contact with the each other.

Inside surface of the combustion chamber is subjected to the heat flux varying with position and time during multiple shots. Corresponding boundary condition is presented in Eq.(7).

$$-\vec{n}\cdot(-k_{barrel}\vec{\nabla}T) = h_{gas}(T_{gas}-T) \quad (7)$$

While the time for inner ballistics is 1.2ms, time interval between two shots is 1s for the investigated 7.62mm barrel [1].

Inner ballistics is a very short time and it is hard to model the phenomena such a very short time. In fact, the temperature of the combustion gases and heat convection coefficient inside the barrel depends on time and position of the projectile during inner ballistics. As time dependent temperature distribution only for the combustion chamber, not for the whole barrel is investigated in this study, gas temperature and heat convection coefficient inside the barrel as a function of position have been used from the study of Işık [12] for the case of 21°C ammunition. They are also presented on Fig. 2. 21°C ammunition condition is one of the NATO standards [13].

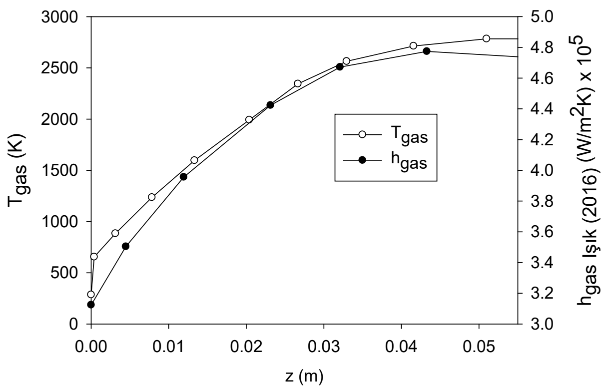

Fig. 2. *Gas temperature and inside heat transfer coefficient form the study of Işık [12]*

As different from other numerical models, in this study gas temperature inside the barrel and inside heat transfer coefficient defined by interpolation function as shown on Fig.3. As it can be seen from Fig. 3, interpolation function rises linearly from 0 to 1 during inner ballistics (1.2m) and decreases linearly from 1 to 0 until the time when second shot starts. Because of this interpolation function defined, heat convection coefficient taken from the study of Işık [12] is not valid in this study. Convenient heat transfer coefficient inside the barrel for this model has been obtained by parametric study, in order to solve this problem. Convenient inside heat transfer coefficient for this study has been obtained as given in Eq. (8).

$$h_{gas} = 2\cdot 10^{-3} h_{gas\ Işık\ (2016)} \quad (8)$$

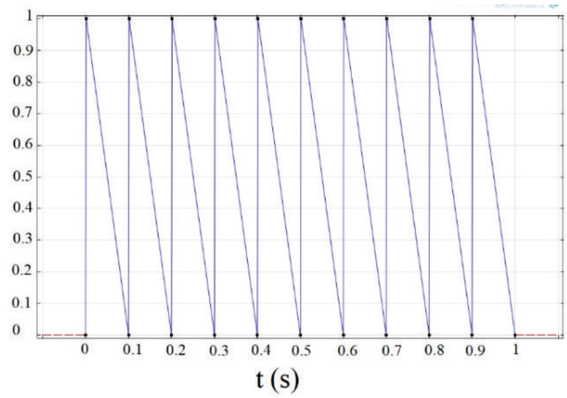

Fig. 3. *Application of interpolation function during successive shots*

Validation of the code has also been shown by Fig.4 by comparing thermal camera measurements on the combustion chamber.

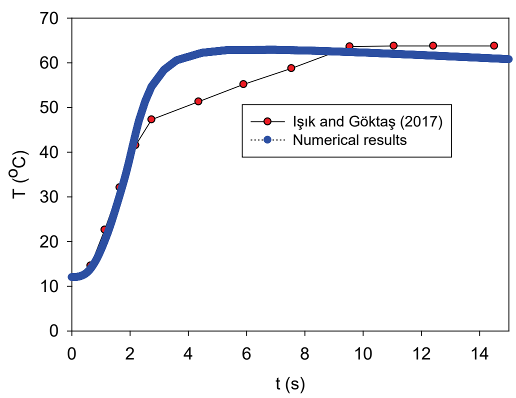

Fig. 4. *Temperature on the combustion chamber (for multiple 20 shots within 2s) [1]*

Mesh dependency analysis for the study was performed as shown in Fig.5. Extremely fine mesh consisting of 6178 triangular elements used in this study.

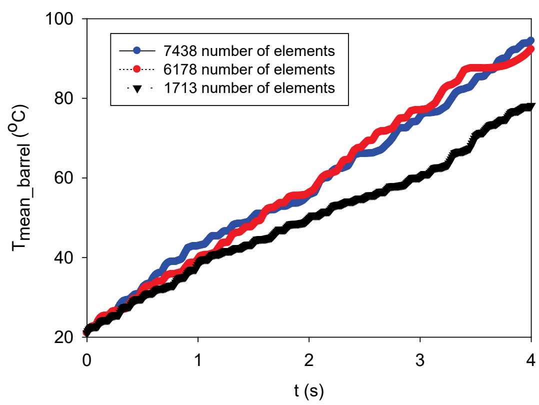

Fig. 5. *Mean temperature of the combustion chamber for successive shots*

RESULTS AND DISCUSSION

The effect of the cartridge thickness t_1 and projectile position inside the cartridge, which is related to L_2, on the cook-off phenomena have been investigated by Comsol Multiphysics and Simulation Software.

Firstly, numerical model has been performed for 80 successive shots only for combustion chamber during 8s. After 8s, cartridge with propellant and projectile at the initial temperature is inserted in the hot combustion chamber, waited for a while until the time when the temperature of the propellant reaches the cook-off temperature, which is 173°C [1]. Fig. 6 shows the temperature simulation at the time when cold cartridge gets in contact with the combustion chamber.

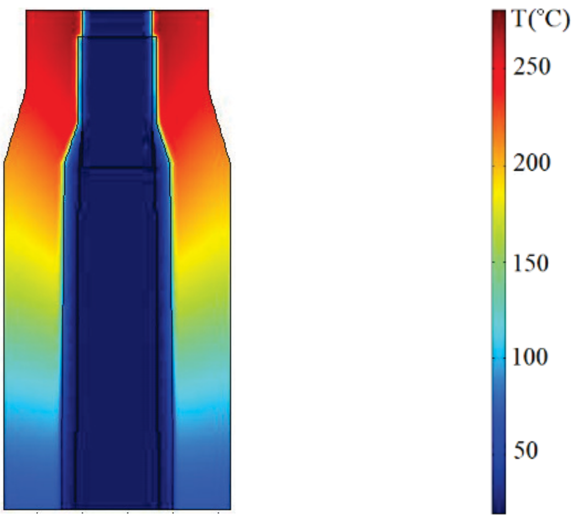

Fig. 6. *Temperature simulation at the t=0s (t_1=1.6mm, L_2=5mm)*

Fig. 7-10 shows heating behavior of the cartridge with propellant and projectile after 10 seconds of getting contact for the investigated cases. Although the maximum temperature in the region of propellant has exceeded cook-off temperature (173°C [1]) at this time, it has been easily observed that generally the hot surface which is in contact with the propellant has higher temperature for the cases of thinner cartridge and front positioning of the projectile. On the other hand, as seen on Fig.8, there are two narrow hot regions in contact with the propellant for the case of t_1=1.6mm, L_2=5mm. It can also be predicted that this increased heat transfer surface will cause cook-off take place previously for this case.

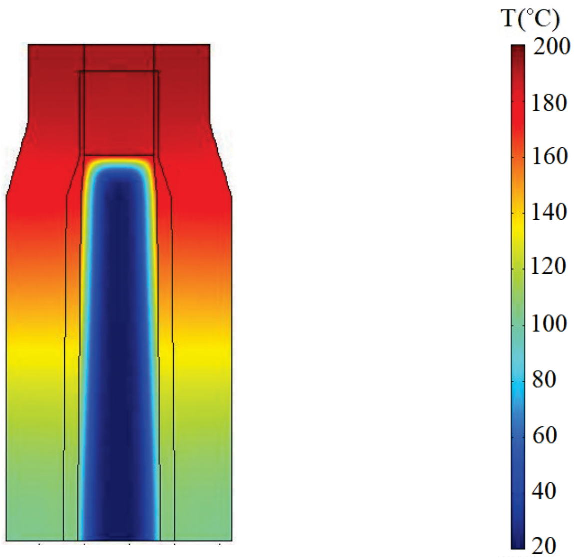

Fig. 7. *Temperature simulation at the t=10s (t_1=1.6mm, L_2=0mm)*

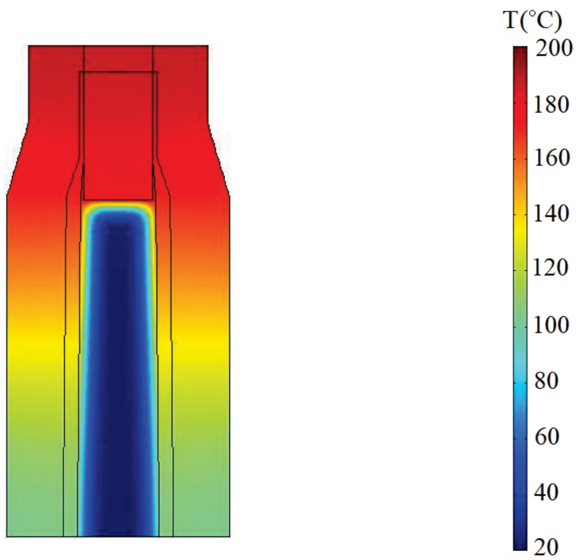

Fig. 8. *Temperature simulation at the t=10s (t_1=1.6mm, L_2=5mm)*

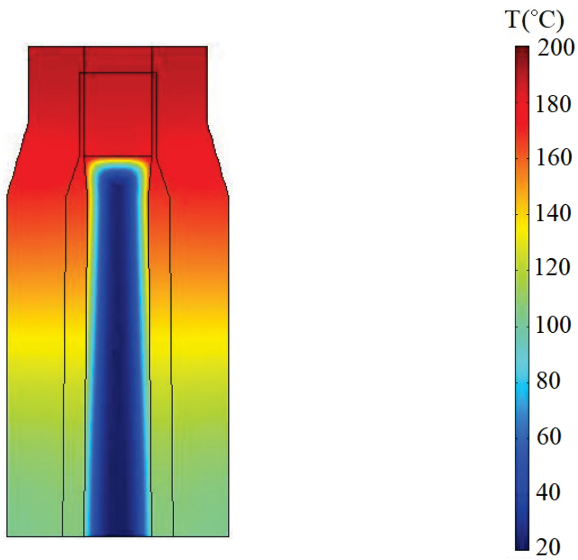

Fig. 9. *Temperature simulation at the t=10s (t_1=2.4mm, L_2=0mm)*

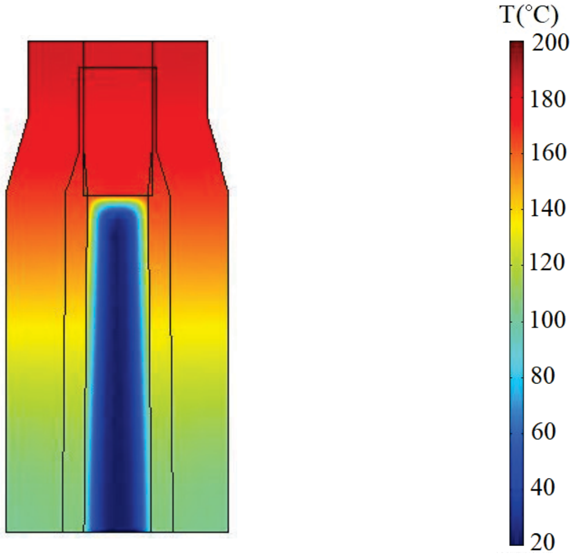

Fig. 10. Temperature simulation at the t=10s (t_1=2.4mm, L_2=5mm)

Cook-off time has been calculated by taking the maximum temperature in the propellant region as a function of time for each cases. The cook-off time and corresponding maximum temperature in the propellant region has been presented in Table 3 for each cases.

Table 3. *Comparison of the investigated cases*

Investigated parameters	cook-off time (s)	T_{max} (°C)
t_1=1.6mm, L_2=5mm	0.09	173.707
t_1=1.6mm, L_2=0mm	0.11	173.480
t_1=2.4mm, L_2=0mm	0.24	173.223
t_1=2.4mm, L_2=5mm	1.34	173.034

CONCLUSION

This study presents the effect the projectile position and the cartridge thickness on the cook-off. Results show that heat transfer area between the hot region and the propellant increases for the case of t_1=1.6mm, L_2=5mm and cook-off starts earlier in this case.

It has also been shown that, regarding the minimum heat transfer surface between the propellant and the hottest region, thicker cartridge and rear positioning of the projectile inside the cartridge prolongs the time for cook-off.

Front side of the cartridge is in contact with the hotter region. Consequently, the design of the front side of the cartridge with projectile positioning is very important factor in order to prevent cook-off.

REFERENCE

[1] Işık H., Göktaş F. Cook-off analysis of a propellant in a 7.62 mm barrel by experimental and numerical methods. Applied Thermal Engineering 2017;112:484–496. https://doi.org/10.1016/j.applthermaleng.2016.10.104.

[2] Mishra A., Hameed A., Lawton BA. Novel scheme for computing gun barrel temperature history and its experimental validation. Journal of Pressure Vessel Technology 2010;132(6):061202-1-6. https://doi.org/10.1115/1.4001740.

[3] Suyadnya KA, Tarwidi D., Setiawan EB, Umbara RF. Numerical modeling of heat transfer in gun barrel with experimental validation. International Journal of Engineering & Technology 2019;8(1.9):62-66. DOI: 10.14419/ijet.v8i1.9.26369.

[4] Akçay M., Yükselen MA., Unsteady thermal studies of gun barrels during the interior ballistic cycle with non-homogenous gun barrel material thermal characteristics. Isı Bilimi ve Tekniği Dergisi (Journal of Thermal Science and Technology) 2014;34(2):75-81.

[5] https://tr.wikipedia.org/wiki/7.62x54mmR

[6] Technical manual, army ammunition data sheets small caliber ammunition FSC 1305, TM 43-0001-27, Headquarters Department of The Army, Washington, D.C., April 1994.

[7] Lawless ZD., Hobbs ML., Kaneshige MJ. Thermal conductivity of energetic materials. Journal of Energetic Materials 2020;38(2):214–239. https://doi.org/10.1080/07370652.2019.1679285.

[8]https://www.alternatewars.com/BBOW/Ballistics/Int/Propellants.htm

[9]http://hyperphysics.phy-astr.gsu.edu/hbase/Tables/thrcn.html

[10] https://en.wikipedia.org/wiki/Lead

[11] https://www.engineeringtoolbox.com/specific-heat-metals-d_152.html

[12] Işık H. Modeling the ballistic parameters in a barrel. Savunma Bilimleri Dergisi (The Journal of Defense Sciences) 2016;15(2):157-177.

[13] Nato standard AEP-97 multi-calibre manual of proof and inspection (M-CMOPI) for Nato small arms ammunition, Edition A Version 1, Nato Standardization Office (NSO), Nato/Otan, October 2020.